Research paper

Dating deep? Luminescence studies of fault gouge from the San Andreas Fault zone 2.6 km beneath Earth's surface

Joel Q.G. Spencer [a,*], Jafar Hadizadeh [b], Jean-Pierre Gratier [c], Mai-Linh Doan [c]

[a] Department of Geology, Kansas State University, Manhattan, KS 66506, USA
[b] Department of Geography and Geosciences, University of Louisville, Louisville, KY 40292, USA
[c] ISTerre, Université Joseph Fourier, Grenoble, France

ABSTRACT

This study aims to assess whether luminescence emission from fault gouge samples from the San Andreas Fault Observatory at Depth (SAFOD) can be used to determine the age distribution of distinct deformation microstructures. Such age determination could help constrain some of the proposed micromechanical models for shear localization in fault gouge, in addition to providing more accurate time constraint on the seismic cycle itself. The mechanism by which previously trapped charge is reset in minerals in fault gouge is thought to be a combination of frictional heating and mechanical deformation, and these processes may be localized to grain surfaces. An added dating complexity specific to deep samples is the high ambient temperature conditions, which act as a barrier to charge storage in lower energy trapping sites. In this work luminescence experiments are being conducted on minerals from whole-rock samples of intact fault gouge from the SAFOD Phase III core. Initial studies indicate (i) the thermal and radiation history of the mineral lattice can be assessed with TL, (ii) trap resetting is evident in both TL and IRSL data, (iii) a small charge-trapping window between drill hole ambient temperature of $\sim$112 °C and higher energy lattice excitation via rupture events is evident in TL data from $\sim$300 to 400 °C, and we tentatively link the source of IRSL to TL within this 300–400 °C region, (iv) IRSL data have low natural intensity but good luminescence characteristics, and (v) SAR IRSL D_e data have high over-dispersion but demonstrate ages ranging from decades to centuries may be measured.

© 2012 Elsevier B.V. All rights reserved.

1. Introduction

One of the interesting issues facing scientists who work with fault gouge is the ability to unravel the age distribution of the different microstructures in the gouge (e.g., clay alteration seams vs. coarser cataclasites, earthquake-related fractures, syntectonic mineral growth; Chester and Chester, 1998; Faulkner et al., 2003). The age distribution of deformation microstructures could help constrain some of the proposed micromechanical models for shear localization in fault gouge, for example identifying the relative effect of stress-driven mass transfer processes (e.g., pressure solution) (Chester and Chester, 1998; Gratier et al., 2011; Holdsworth et al., 2011; Janssen et al., 2011) vs. friction-controlled processes (Carpenter et al., 2011; Lockner et al., 2011) in active creeping zones. Presently, the only reliable tool for such analysis is the use of cross-cutting relationships (e.g., Lin et al., 2001; Chester et al., 1993), for example the observation, in creeping zones, of cross-cutting

cleavages (Gratier et al., 2011), cross-cutting veins (Mittempergher et al., 2011), or deformed clasts embedded in such creeping zones (Hadizadeh et al., in press), although a limited number of studies have attempted to determine the absolute age of gouge components. Among these studies include the application of trapped charge dating techniques to fault gouge minerals. The mechanism by which previous trapped charge may be reset in minerals in fault gouge is thought to be either frictional heating or mechanical deformation, or a combination of these. Additionally, these processes may be localized to grain surfaces (Takeuchi et al., 2006).

Only a handful of luminescence studies have attempted to directly date active faults by studying either liquefaction features (e.g., Banerjee et al., 1997; Porat et al., 2007; Thomas et al., 2007) or fault gouge (e.g., Singhvi et al., 1994; Ding and Lai, 1997; Banerjee et al., 1999; Mukul et al., 2007). Despite consistent TL and radiocarbon ages (Singhvi et al., 1994) and agreement between TL and infrared stimulated luminescence (IRSL) data (Banerjee et al., 1999), the resetting of the luminescence signal in fault gouge is often doubted. Some studies indicate no evidence for resetting in fault gouge (e.g., Fukuchi and Imai, 1998; Toyoda et al., 2000), while

* Corresponding author. Tel.: +1 785 532 2249; fax: +1 785 532 5159.
E-mail address: joelspen@ksu.edu (J.Q.G. Spencer).

others suggest a grain size dependence with finest grains most likely reset (e.g., Rink et al., 1999; Ulusoy, 2004; Takeuchi et al., 2006).

The availability of samples from the NSF EarthScope San Andreas Fault Observatory at Depth (SAFOD) Phase III drilling provides a unique opportunity to study luminescence properties of fault gouge from the well-documented seismically active sections of the San Andreas Fault zone, where the drill well casing is currently being deformed by fault creep. Notwithstanding the challenges to luminescence dating of deep SAFOD samples such as high ambient temperature conditions due to geothermal gradient, adequate resetting, and possible highly fractured mineral grains, age determination of fault gouge has an important contribution to understanding earthquake mechanics and as an earthquake predictive tool. The SAFOD experiment presents an ideal laboratory to study small-scale temporal resolution of comminution due to creep motion as well as numerous episodes of earthquake rupture. The aim of this work is to assess whether luminescence emission from fault gouge samples from the SAFOD can be used to determine the age distribution of distinct deformation microstructures. Our approach in this preliminary study was to measure grains from disaggregated rock slices. In future work we aim to investigate methods of surface dating of intact samples (e.g., Greilich et al., 2005) which have the advantage of spatially resolving equivalent dose (D_e) and dose-rate data and matching these grain-for-grain to accurately assess age data from the sample surface.

2. SAFOD sample description

A sample of SAFOD core material from Hole E, Run 1, Section 2 (E12) (http://www.earthscope.org/data/safod_core_viewer) of Phase III of the drilling program was obtained for luminescence analyses. The sample was an intact cuboid sectioned from a larger sample #3, originally obtained by the Gratier/Hadizadeh groups. The sample had dimensions of $\sim 23 \times 19 \times 16$ mm, with a complex assemblage of mm-sized minerals and a small fault clearly visible. The measured depth (MD) or depth along the drill core at the sample position was 3143 m. The true vertical depth (TVD) was 2604 m below the surface. At this locality the ambient temperature is estimated to be ~ 112 °C. This value is obtained from a combination of extrapolated borehole temperatures (Williams et al., 2005; Schleicher et al., 2008) and thermal gradient values. Thin section SEM analyses performed by the Gratier group specifically on this sample and on further samples from the SAFOD damaged zone and from the two main creeping zones (Gratier et al., 2011; Hadizadeh et al., in press) show that the mineral assemblage is a mixture of quartz, K-feldspar, Na–Ca-feldspar, calcite, chlorite-mica phyllosillicates, Fe and Ti oxides, and pyrite.

3. Luminescence studies

3.1. Sample preparation

Sample preparation was carried out under very low intensity ~ 590 nm lighting to minimize removal of luminescence signals from quartz and feldspar minerals. Investigations deliberately focused on the half of the sample not cut by the small fault (Fig. S1), leaving the side intersected by the fault intact for future measurements. A slow-speed water-cooled rock saw was used to sub-sample the SAFOD sample. Slices of ~ 2 mm thickness were removed from the exterior surfaces (Fig. S1B). This was done to minimize any prior optical (laboratory white lights or daylight) or thermal (from previous rock sawing) reduction of luminescence from the sample (Fig. S2). The interior stub was then sliced into four ~ 2 mm slices (Fig. S1C). Slice F4, from the interior closest to the

center of the sample, and F3 the next slice in sequence were chosen for grain preparation for luminescence analyses. Exterior slice D0-1 (~ 0.5 g) was prepared to provide preliminary dosimetry data. This slice was crushed to a fine powder using an agate mortar and pestle in preparation for ICPMS and ICPOES elemental analyses.

Slices F3 and F4 were very gently disaggregated; applying pressure between finger and thumb was sufficient to release grains from the slice matrix. The samples were sieved to obtain a 175–250 μm grain size fraction and washed in 10% HCl acid. The resulting sieve fractions were subdivided to produce polymineral (no further treatment), K-rich feldspar (<2.58 g cm^{-3} lithium metatungstate, LMT), and etched K-rich feldspar (<2.58 g cm^{-3} LMT and 40 min 10% HF wash). Silkospray and spray templates were used to mount aliquots of grains 3 mm in diameter on stainless steel discs. Due to the small sample size grain yields were generally very low, particularly for the un-etched and etched K-feldspar, for which only 15 and 2 aliquots were prepared, respectively.

3.2. Measurements

Luminescence measurements were made using a Risø TL/OSL-DA-20 automated reader (Bøtter-Jensen et al., 2003). Optical stimulation used 870Δ40 nm infrared diodes at ~ 117.9 mW cm^{-2} (22 Vishay TSFF5200 at 90% power) while holding the sample at 50 °C. All TL measurements were carried out with a heating rate of 50 °C s^{-1}. A calibrated ^{90}Sr/^{90}Y beta source (~ 0.16 Gy s^{-1}) was used to administer laboratory radiation doses. All luminescence signals were detected in the near-UV to blue spectral range (335–440 nm at 50% transmission; 320–470 nm at 10% transmission) using 2 mm Schott BG-39 and 4 mm Corning 7–59 filters with an EMI 9235QB photomultiplier tube. The etched K-feldspar grains showed no natural IRSL shinedown, so further measurements concentrated on the polymineral and un-etched K-feldspar grains.

3.3. Resetting and potential traps for dating

Aliquots of polymineral grains from slice F4 were used to investigate possibilities of luminescence resetting. Some exploratory sequential IRSL then TL measurements were conducted. The natural IRSL signal (Fig. S3) is weak and could correspond to a small proportion of trapped charge, poor luminescence sensitivity, or absence of suitable grains for IRSL. In contrast, IRSL from the same
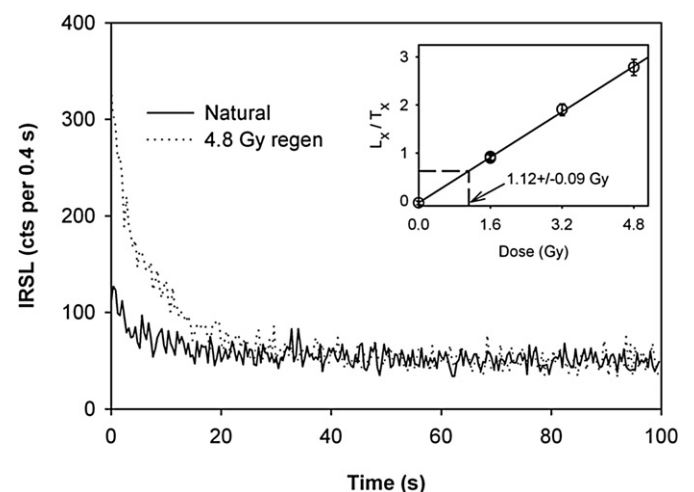

Fig. 1. IRSL signals from a 3-mm aliquot of 175–250 μm un-etched K-feldspar from slice F4 (disc SAF-F408-3). Inset: SAR IRSL growth curve for the same aliquot.

aliquot subsequent to ~16 Gy beta has a more familiar decay (Fig. S3). Un-etched K-feldspar aliquots show similar characteristics (Fig. 1). These qualitative observations possibly suggest the natural IRSL does correspond to a relatively small proportion of trapped charge and may therefore indicate resetting by a past rupture event.

Corresponding TL data for the polymineral grains is shown in Fig. 2. The ratio of natural-to-artificial TL indicates that the natural TL peak rising rapidly after ~400 °C represents a large residual dose, corresponding to a value in excess of ~16 Gy. Between ~300 to 400 °C in the natural TL signal a small peak is present; this small peak represents a dose perhaps 1–2 orders of magnitude lower than the large residual. We expect the ratio of natural-to-artificial TL to rise in this temperature region because the small peak is accumulating on the tail of the large residual. These data may suggest the following interpretations: a past rupture event is associated with the initial rise of the large residual (cf. for thermal
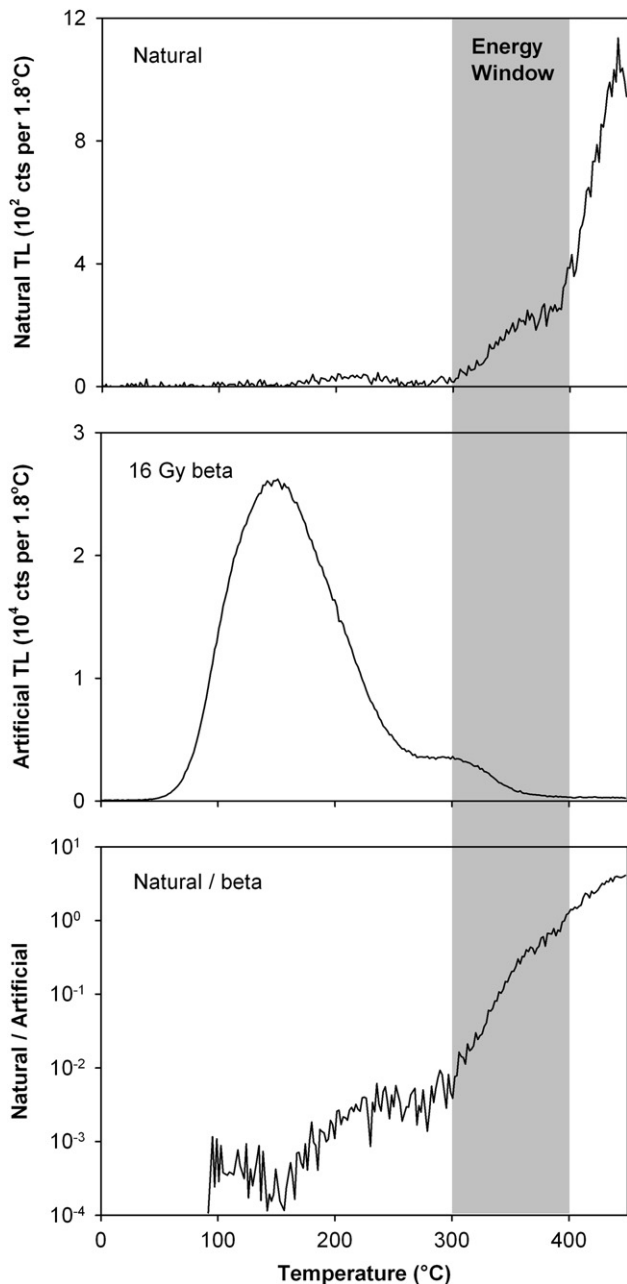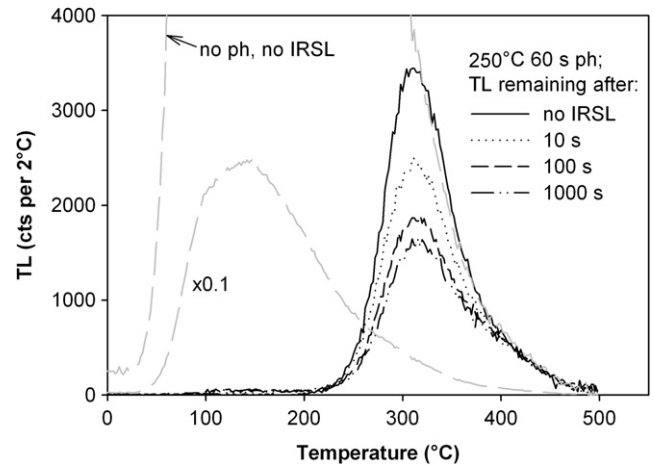

Fig. 3. Effect of prior IR on TL. An aliquot of un-etched K-feldspar from slice F3 was heated to 500 °C, given a dose of ~75 Gy, preheated to 250 °C for 60 s, exposed to IR for times indicated, and TL measured to 500 °C. Reproducibility was checked by repeating the first (0 s IR) measurement (TL curve not shown). Data subsequent to preheat and IR exposure are compared to TL measured from the same aliquot after the same beta dose but without preheat or IR exposure (gray dashed line).

exposure in Spencer and Sanderson, 1994, in press) and has removed TL to ~400 °C; charge has subsequently accumulated in traps corresponding to TL <400 °C, but this trapping is in competition with ~112 °C eviction. Depending on the duration of ~112 °C eviction, a small energy window is available for trapping datable charge.

From our observation of the low intensity natural IRSL signal (Fig. S3 and Fig. 1) we suspect that the small energy window available for trapping charge for TL may also trap charge that can be stimulated by IR exposure. To explore the relationship between IRSL and TL further the effect of prior IR on TL after preheating was examined on an un-etched K-feldspar aliquot of F3, in a comparable experiment to Murray et al. (2009). The results of this experiment in Fig. 3 show significant IR depletion of the annealed TL at ~315 °C; in the TL data without preheating or IR exposure clearly identifiable peaks are absent. Murray et al. (2009) observe the most significant IR effect on their recognizable TL peak at ~410 °C, and tentatively identify the source of IRSL with this TL peak.

The ~410 °C peak is absent in our data, but in contrast a possible link between IRSL source and the annealed TL "peak" at ~315 °C is indicated. This is consistent with the energy window between ~300 to 400 °C (Fig. 2), and we believe this relationship may still persist at
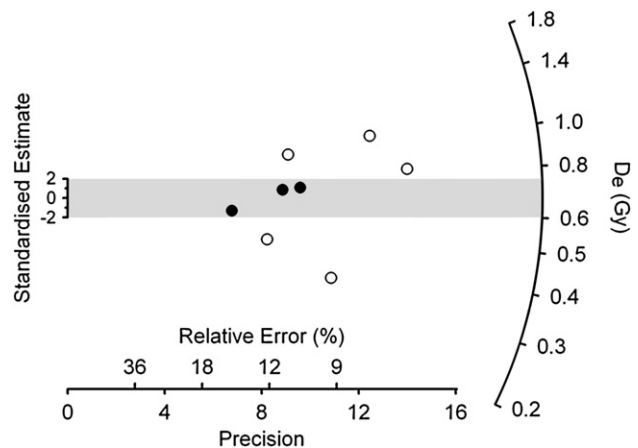

Fig. 2. TL signals from a 3-mm aliquot of 175–250 μm polymineral grains from slice F4.

Fig. 4. Radial plot of D_e data from K-feldspar aliquots from slice F4. 2-sigma band positioned on Central Age Model result.

Table 1
Measured elemental concentrations of U, Th, Rb from ICPMS and K_2O from ICPOES, and calculated total dose-rate for 175–250 μm un-etched K-rich feldspar.

Sample	Crushed slice[a]	U (ppm)	Th (ppm)	Rb (ppm)	K_2O^b (%)	Dose-rate[c] (mGy a^{-1})
SAFOD-3	D0-1	1.70 ± 0.26	5.90 ± 0.59	118 ± 11.8	3.67 ± 0.18	4.81 ± 0.40

[a] Sampling details in Section 3.1 and Fig. S1C.
[b] Converted to K% by atomic abundance.
[c] Measured moisture content and calculated dose-rate due to cosmic rays were negligible. Internal K was taken as 12.5% (after Huntley and Baril, 1997) $\pm5\%$ and internal Rb of $0.035 \pm 0.015\%$ (from Aitken, 1998, p. 42) using absorbed dose fractions after Mejdahl (1979). Negligible internal alpha dose was assumed. Alpha efficiency for external alpha was taken as 0.2 ± 0.1 (consistent with Balescu and Lamothe, 1994; Duller et al., 1995). Dose-rate conversion factors from Adamiec and Aitken (1998).

preheats higher than 250 °C or for preheating duration greater than 60 s. The relationship between IRSL and TL in these samples will be explored in more detail in future work. For the purposes of this study, further examination of dating feasibility concentrated on IRSL signals and is discussed in the following section.

3.4. Toward dating of K-feldspar single aliquots

A single-aliquot regenerative-dose (SAR) procedure similar to Martins et al. (2010) was used to investigate the suitability of un-etched K-rich feldspar from the F4 slice for IRSL dating. This SAR procedure used a preheat of 250 °C for 60 s, a test-dose of 1.6 Gy, regenerative and test-dose IRSL measurements for 100 s at 50 °C, and an IRSL hotbleach for 40 s at 290 °C. Dose recovery test data and equivalent dose (D_e) data were generated using this procedure.

The natural IRSL of the K-feldspar has low intensity but good response to a 4.8 Gy regenerative dose (Fig. 1). The dose response is linear with good recycling and low recuperation characteristics (Fig. 1, inset). Dose recovery tests were promising with 3 out of 4 aliquots tested able to recover known dose within 10% tolerance limits (Fig. S4).

Eight SAR IRSL D_e values were measured from K-feldspar from slice F4. These are shown on a radial plot (Galbraith, 1990) in Fig. 4. The data show quite a degree of scatter, which could be due to the influence of successive rupture events, a heterogeneous radiation field, variation in signal stability, or partial resetting. If a single rupture event is assumed, the Central Age Model (Galbraith et al., 1999) gives a D_e of 0.67 ± 0.10 Gy with σ_b of 42%.

Dose-rate from ICP analyses of crushed slice D0-1 suggests a value of 4.81 ± 0.40 mGy a^{-1} (Table 1), resulting in an OSL age of 139 ± 12 years before 2010. Because of small sample size, heterogeneity of grain matrix, and various assumptions used in the calculation, the dose-rate assessment can only be viewed as approximate but is a reasonable working value to allow estimation of possible age range that can be measured. The largest historical $M_W7.9$ Fort Tejon earthquake occurred in 1857, and there is a possibility that even at this early stage of our investigations the IRSL data could match this date. Furthermore, the small doses involved add support to a link between the small charge-trapping window identified in TL data with the source of measured IRSL.

A further consideration is that charge accumulating in the IRSL trap(s) may be depleted by the ~ 112 °C isothermal, and hence whether the 250 °C 60 s preheat is sufficient to anneal the natural IRSL. This was tested with K-feldspar aliquots of F3 with the 250 °C 60 s preheat and a higher preheat of 290 °C for 60 s. These preliminary data are consistent with the F4 results (Fig. 4) and suggest, albeit at an early stage of exploratory measurements, that any imbalance between natural and regenerative charge may have a small or negligible effect on D_e.

4. Conclusions

In this study we have investigated IRSL and TL properties of polymineral and K-feldspar aliquots extracted from a small sample of fault gouge from SAFOD drill core. Initial studies indicate (i) the thermal and radiation history of the mineral lattice can be assessed with TL, (ii) trap resetting is evident in both TL and IRSL data, (iii) a small charge-trapping window between drill hole ambient temperature of ~ 112 °C and higher energy lattice excitation via rupture events is evident in TL data from ~ 300 to 400 °C, and we tentatively link the source of IRSL to TL within this 300–400 °C region, (iv) IRSL data have low natural intensity but good luminescence characteristics, and (v) SAR IRSL D_e data have high over-dispersion but demonstrate ages ranging from decades to centuries may be measured.

Appendix A. Supporting information

Supplementary data associated with this article can be found, in the online version, at doi:10.1016/j.quageo.2012.04.023.

References

Adamiec, G., Aitken, M.J., 1998. Dose-rate conversion factors: update. Ancient TL 16, 37–50.
Aitken, M.J., 1998. An Introduction to Optical Dating. Oxford University Press.
Balescu, S., Lamothe, M., 1994. Comparison of TL and IRSL age estimates of feldspar coarse grains from waterlain sediments. Quaternary Geochronology (Quaternary Science Reviews) 13, 437–444.
Banerjee, D., Singhvi, A.K., Bagati, T.N., Mohindra, R., 1997. Luminescence chronology of seismites in Sumdo (Spiti valley) near Kaurik-Chango Fault, Northwestern Himalaya. Current Science 73, 276–281.
Banerjee, D., Singhvi, A.K., Pande, K., Gogte, V.D., Chandra, B.P., 1999. Towards a direct dating of fault gouges using luminescence dating techniques – methodological aspects. Current Science 77, 256–268.
Bøtter-Jensen, L., Andersen, C.E., Duller, G.A.T., Murray, A.S., 2003. Developments in radiation, stimulation and observation facilities in luminescence measurements. Radiation Measurements 37, 535–541.
Carpenter, B.M., Marone, C., Saffer, D.M., 2011. Weakness of the San Andreas Fault revealed by samples from the active fault zone. Nature Geoscience 4, 251–254.
Chester, F.M., Chester, J.S., 1998. Ultracataclasite structure and friction processes of the Punchbowl fault, San Andreas system, California. Tectonophysics 295, 199–221.
Chester, F.M., Evans, J.P., Biegel, R.L., 1993. Internal structure and weakening mechanisms of the San Andreas Fault. Journal of Geophysical Research 98, 771–786.
Ding, Y.Z., Lai, K.W., 1997. Neotectonic fault activity in Hong Kong: evidence from seismic events and thermoluminescence dating of fault gouge. Journal of the Geological Society, London 154, 1001–1007.
Duller, G.A.T., Wintle, A.G., Hall, A.M., 1995. Luminescence dating and its application to key pre-late Devensian sites in Scotland. Quaternary Science Reviews 14, 495–519.

Faulkner, D.R., Lewis, A.C., Rutter, E.H., 2003. On the internal structure and mechanics of large strike-slip fault zones: field observations of the Carboneras fault in southeastern Spain. Tectonophysics 367, 235–251.

Fukuchi, T., Imai, N., 1998. Resetting experiment of E' centres by natural faulting – the case of the Nojima earthquake fault in Japan. Quaternary Science Reviews 17, 1063–1068.

Galbraith, R.F., 1990. The radial plot: graphical assessment of spread in ages. Nuclear Tracks and Radiation Measurements 17, 197–206.

Galbraith, R.F., Roberts, R.G., Laslett, G.M., Yoshida, H., Olley, J.M., 1999. Optical dating of single and multiple grains of quartz from Jinmium rock shelter, northern Australia: part I, experimental design and statistical models. Archaeometry 41, 339–364.

Gratier, J.-P., Richard, J., Renard, F., Mittempergher, S., Doan, M.-L., Di Toro, G., Hadizadeh, J., Boullier, A.-M., 2011. Aseismic sliding of active faults by pressure solution creep: evidence from the San Andreas Fault observatory at depth. Geology 39 (12), 1131–1134.

Greilich, S., Glasmacher, U.A., Wagner, G.A., 2005. Optical dating of granitic stone surfaces. Archaeometry 47, 645–665.

Hadizadeh, J., Mittempergher, S., Gratier, J.-P., Renard, F., Di Toro, G., Richard, J., Babaie, H.A. A microstructural study of fault rocks from the SAFOD: implications for the deformation mechanisms and strength of the creeping segment of the San Andreas Fault. Journal of Structural Geology, in press.

Holdsworth, R.E., van Diggelen, E.W.E., Spiers, C.J., de Bresser, J.H.P., Walker, R.J., Bowen, L., 2011. Fault rocks from the SAFOD core samples: implications for weakening at shallow depths along the San Andreas Fault, California. Journal of Structural Geology 33, 132–144.

Huntley, D.J., Baril, M.R., 1997. The K content of the K-feldspars being measured in optical and thermoluminescence dating. Ancient TL 15, 11–13.

Janssen, C., Wirth, R., Reinicke, A., Rybacki, E., Naumann, R., Wenk, H.-R., Dresen, G., 2011. Nanoscale porosity in SAFOD core samples (San Andreas Fault). Earth and Planetary Science Letters 301, 179–189.

Lin, A., Shimamoto, T., Maruyama, T., Sigetomi, M., Miyata, T., Takemura, T., Tanaka, H., Uda, S., Murata, A., 2001. Comparative study of cataclastic rocks from a drill core and outcrop of the Nojima Fault zone on Awaji Island, Japan. Island Arc 10, 368–380.

Lockner, D.A., Morrow, C., Moore, D.E., Hickman, S., 2011. Low strength of deep San Andreas Fault gouge from SAFOD core. Nature 472, 82–85.

Martins, A.A., Cunha, P.P., Buylaert, J.-P., Huot, S., Murray, A.S., Dinis, P., Stokes, M., 2010. K-feldspar IRSL dating of a Pleistocene river terrace staircase sequence of the Lower Tejo River (Portugal, western Iberia). Quaternary Geochronology 5, 176–180.

Mejdahl, V., 1979. Thermoluminescence dating: beta attenuation in quartz grains. Archaeometry 21, 61–72.

Mittempergher, S., Di Toro, G., Gratier, J.-P., Hadizadeh, J., Smith, S.A.F., Spiess, R., 2011. Evidence of transient increases of fluid pressure in SAFOD phase III cores. Geophysical Research Letters 38, L03301.

Mukul, M., Jaiswal, M., Singhvi, A.K., 2007. Timing of recent out-of-sequence active deformation in the frontal Himalayan wedge: insights from the Darjiling sub-Himalaya, India. Geology 35, 999–1002.

Murray, A.S., Buylaert, J.P., Thomsen, K.J., Jain, M., 2009. The effect of preheating on the IRSL signal from feldspar. Radiation Measurements 44, 554–559.

Porat, N., Levi, T., Weinberger, R., 2007. Possible resetting of quartz OSL signals during earthquakes – evidence from late Pleistocene injection dikes, Dead Sea Basin, Israel. Quaternary Geochronology 2, 272–277.

Rink, W.J., Toyoda, S., Rees-Jones, J., Schwarcz, H.P., 1999. Thermal activation of OSL as a geothermometer for quartz grain heating during fault movements. Radiation Measurements 30, 97–105.

Schleicher, A.M., War, L.N., van der Pluijm, B.A., 2008. The geological significance of mixed-layered clay minerals in the San Andreas Fault observatory at depth (SAFOD) drillhole in Parkfield, California. Geotectonic Research 95, 160–162.

Singhvi, A.K., Banerjee, D., Pande, K., Gogte, V., Valdiya, K.S., 1994. Luminescence studies on neotectonic events in south-central Kumaun Himalaya – a feasibility study. Quaternary Science Reviews (Quaternary Geochronology) 13, 595–600.

Spencer, J.Q., Sanderson, D.C.W., 1994. Mapping thermal exposure by luminescence thermometry. Radiation Measurements 23, 465–468.

Spencer, J.Q.G., Sanderson, D.C.W. Decline in firing technology or poorer fuel resources? High-temperature thermoluminescence (HTTL) archaeothermometry of Neolithic ceramics from Pool, Sanday, Orkney. Journal of Archaeological Sciences, in press.

Takeuchi, A., Nagahama, H., Hashimoto, T., 2006. Surface resetting of thermoluminescence in milled quartz grains. Radiation Measurements 41, 826–830.

Thomas, P.J., Reddy, D.V., Kumar, D., Nagabhushanam, P., Sukhija, B.S., Sahoo, R.N., 2007. Optical dating of liquefaction features to constrain prehistoric earthquakes in Upper Assam, NE India – some preliminary results. Quaternary Geochronology 2, 278–283.

Toyoda, S., Rink, W.J., Schwarcz, H.P., Rees-Jones, J., 2000. Crushing effects on TL and OSL on quartz: relevance to fault dating. Radiation Measurements 32, 667–672.

Ulusoy, U., 2004. ESR dating of North Anatolian (Turkey) and Nojima (Japan) faults. Quaternary Science Reviews 23, 161–174.

Williams, C.F., D'Alessio, M.A., Grubb, F.V., Galanis, S.P., 2005. Heat Flow Studies in the SAFOD Main Hole. American Geophysical Union, Fall Meeting 2005, abstract #T23E-07.